

Stabilized collagen matrix dressing improves wound macrophage function and epithelialization

Mohamed S. El Masry,^{*,†,‡} Scott Chaffee,[†] Piya Das Ghatak,^{*,†} Shomita S. Mathew-Steiner,^{*,†} Amitava Das,^{*,†} Natalia Higueta-Castro,[†] Sashwati Roy,^{*,†} Raafat A. Anani,[‡] and Chandan K. Sen^{*,†,1}

^{*}Department of Surgery, Indiana University Health (IUH) Comprehensive Wound Center, Indiana Center for Regenerative Medicine and Engineering, Indiana University School of Medicine, Indianapolis, Indiana, USA; [†]Department of Surgery, The Ohio State University, Wexner Medical Center, Columbus, Ohio, USA; and [‡]Department of Plastic and Reconstructive Surgery, Zagazig University, Zagazig, Egypt

ABSTRACT: Decellularized matrices of biologic tissue have performed well as wound care dressings. Extracellular matrix–based dressings are subject to rapid degradation by excessive protease activity at the wound environment. Stabilized, acellular, equine pericardial collagen matrix (sPCM) wound care dressing is flexible cross-linked proteolytic enzyme degradation resistant. sPCM was structurally characterized utilizing scanning electron and atomic force microscopy. In murine excisional wounds, sPCM was effective in mounting an acute inflammatory response. Postwound inflammation resolved rapidly, as indicated by elevated levels of IL-10, arginase-1, and VEGF, and lowering of IL-1 β and TNF- α . sPCM induced antimicrobial proteins S100A9 and β -defensin-1 in keratinocytes. Adherence of *Pseudomonas aeruginosa* and *Staphylococcus aureus* on sPCM pre-exposed to host immune cells *in vivo* was inhibited. Excisional wounds dressed with sPCM showed complete closure at d 14, while control wounds remained open. sPCM accelerated wound re-epithelialization. sPCM not only accelerated wound closure but also improved the quality of healing by increased collagen deposition and maturation. Thus, sPCM is capable of presenting scaffold functionality during the course of wound healing. In addition to inducing endogenous antimicrobial defense systems, the dressing itself has properties that minimize biofilm formation. It mounts robust inflammation, a process that rapidly resolves, making way for wound healing to advance.—El Masry, M. S., Chaffee, S., Das Ghatak, P., Mathew-Steiner, S. S., Das, A., Higueta-Castro, N., Roy, S., Anani, R. A., Sen, C. K. Stabilized collagen matrix dressing improves wound macrophage function and epithelialization. *FASEB J.* 33, 2144–2155 (2019). www.fasebj.org

KEY WORDS: antimicrobial peptides · ECM · scaffold · biofilm · cytokines

Breach of skin integrity is the primary hallmark of cutaneous injury. To cover the opening thus caused, wound care dressings are placed in contact with the wound. The primary purposes of the dressing are to cover the skin defect, thus protecting the injured and underlying tissue from infection. Although wound occlusion was indeed the primary purpose of wound care dressings historically (1–3), expectations evolved over time. In the 19th century, the notion of infection management was introduced (4, 5). In the 1980s, wound care dressings aimed at keeping the wound moist and absorbing fluids. Polyurethane foams, iodine-containing gels, and hydrocolloids and other such matrices were then introduced. In the 1990s, the wound care dressing product range vastly

expanded to include silicone meshes, tissue adhesives, vapor-permeable adhesive films, and collagen-containing material (6–8). Today, wound care dressings are designed to actively influence the wound repair process such that inflammation may be resolved in a timely manner, making way for adequate wound tissue vascularization and rapid closure (9–11). Importantly, it is now recognized that covering the wound with skin and lack of discharge is no longer sufficient to claim wound closure. Evidence supporting wound closure must document that the repaired skin has acquired intact barrier function (12, 13). Repaired skin, deficient in barrier function, is viewed as faulty closure that may result in wound recurrence (14, 15).

Naturally derived biomaterials such as decellularized matrix of biologic tissue have performed well as wound care dressings. Such dressings demonstrate immunomodulatory properties and can modify host response (16, 17). In addition, such dressings present the advantage of native extracellular matrix (ECM) (18). However, the challenge faced by any ECM-based wound care dressing product is its rapid degradation by the excessive matrix metalloproteinases and other proteases present in the wound environment. Pericardium is a matrix dense tissue composed of many of the same

ABBREVIATIONS: AFM, atomic force microscopy; AMP, antimicrobial peptide; ECM, extracellular matrix; HBD, human β -defensin; IVIS, *in vivo* imaging system; PC, polycarbonate membrane; SEM, scanning electron microscopy; sPCM, stabilized acellular equine pericardial collagen matrix

¹ Correspondence: Indiana University School of Medicine, 975 W. Walnut St., Medical Research Library Building, Suite 454, Indianapolis, IN 46202, USA. E-mail: cksen@iu.edu

doi: 10.1096/fj.201800352R

This article includes supplemental data. Please visit <http://www.fasebj.org> to obtain this information.

proteins and glycans as vascular tissue, including the proteins collagen, elastin, fibrillin, and fibronectin (19). Additionally, pericardium is sparsely cellularized, making it a suitable candidate to donate xenographic tissue. Light DNA content of this tissue can be easily removed (20, 21). The equine pericardium biomatrix has been used in clinics for different wound types, including diabetic ulcers (22, 23). It is commercialized as stabilized acellular equine pericardial collagen matrix (sPCM) wound care dressing. Derived from equine pericardium, the natural collagen structure is preserved in sPCM. This is achieved by a decellularization process, followed by stabilization (cross-linking) and sterilization with ethylene dichloride. The final product is a proteolytic enzyme degradation resistant, fully flexible cross-linked tissue that may be used as wound care dressing (24). A bridge stabilization process preserves the biomechanics and biocompatibility of sPCM, affording resistance to enzymatic degradation at the wound site rich in matrix metalloproteinases and other proteases. A single-application regimen makes it simple to administer and economical (25, 26). In this work, we sought to understand the mechanism of action of sPCM as a wound care dressing.

MATERIALS AND METHODS

Animal and experimental design

Male C57BL/6 mice were obtained from Harlan Laboratory (Indianapolis, IN, USA). All animals were 8 wk old at the start of the experiment. Mice were randomly (<https://www.random.org/>) divided into different groups as indicated in the corresponding figure legends (Supplemental Fig. S1). Briefly, the dorsal side of the mice was removed of hair and cleaned using povidone-iodine under anesthesia. During the procedure, mice were anesthetized by low-dose isoflurane inhalation. Two rectangular (8 × 16 mm) full-thickness excisional wounds were made on the dorsal skin, followed by applying the sPCM (Harbor MedTech, Irvine, CA, USA) according to the manufacturer's instructions. The dressing was cut to the size of the wound after soaking it with sterile saline for 3 min and then secured to the wound edges on 1 side using interrupted 5-0 nylon sutures (Ethicon, Somerville, NJ, USA). Care was taken to ensure that the dressing was in complete contact with the wound bed. The other side of dorsal wound was covered with semiocclusive dressing (Tegaderm; 3M, St. Paul, MN, USA). Then secondary dressing was applied for both wounds. sPCM was maintained on the wound until the material fell off or became completely dry (nonviable). Animals were euthanized at specific times, and wound tissues were collected for molecular and histologic analyses. The Ohio State University Institutional Animal Care and Use Committee approved all animal experiments.

Wound area planimetry

Wound imaging was performed at d 0 and 14 by using a digital camera (Canon Power Shot S6; Melville, NY, USA), and the wound area was calculated by ImageJ software (Image Processing and Analysis in Java; National Institutes of Health, Bethesda, MD, USA; <https://imagej.nih.gov/ij/>) (27).

Isolation of murine wound macrophages

To collect live wound macrophages, circular 8 mm sponges were taken from a sterile polyvinyl alcohol disc and sterilized in

boiling ddH₂O. Polycarbonate membrane (PC) and sPCM were implanted between 2 sponges and sutured together. Two PC sponges were implanted subcutaneously on the back of 8 wk old C57BL/6 mice, with 2 sPCM on the opposite side of the midline. Macrophages were isolated from the sponges *via* compression in sterile PBS and CD11b magnetic sorting as previously described (27, 28).

Efferocytosis and immunocytochemistry

Apoptotic cell clearance assay was conducted using wound macrophages cocultured with thymocytes *ex vivo*, as previously described (27, 28). In brief, CD11b-selected wound macrophages were cocultured for 1 h at 37°C in 8-well chambered slides with apoptotic (5 mM dexamethasone treated) thymocytes previously labeled with pHrodo Red succinimidyl ester (P36600; Thermo Fisher Scientific, Waltham, MA, USA) for 12 h. Cells were washed in medium to remove excess nonengulfed cells. Cells were fixed with fixation buffer (00-8222-49; eBioscience, San Diego, CA, USA) and stained using rat anti-mouse F4/80 (MCA497; Bio-Rad, Hercules, CA, USA). Chamber slides were imaged using a Zeiss Axio-scanner (Carl Zeiss GmbH, Jena, Germany). Efferocytosis index was calculated by the number of engulfed apoptotic thymocytes per macrophage in various fields of view (27, 28).

Cell culture

Immortalized human keratinocytes (HaCaT) cells were grown in Dulbecco low-glucose modified Eagle medium (11885-092; Thermo Fisher Scientific) as previously described (29). Cells were maintained in a standard culture incubator with humidified air containing 5% CO₂ at 37°C. Cells were seeded on sPCM and incubated for 24 h. Cell seeded on regular cell culture grade plastic wells were used as controls.

Bacterial strain and culture

For the IVIS experiment, *Pseudomonas aeruginosa* (Xen41; base strain PA01; PerkinElmer, Waltham, MA, USA) or *Staphylococcus aureus* (SAP231; base strain USA300; PerkinElmer) were used. These stably luminescent clinical strains contain integrated plasmids carrying a luciferase gene that is constitutively expressed. PA01 were cultured in low salt Luria-Bertani broth (Thermo Fisher Scientific). SAP231 were cultured in tryptic soy broth. Bioluminescent bacteria only produce light when they are alive and metabolically active. Thus, we used light emission as detected with the IVIS system (PerkinElmer) as an indicator of bacterial activity. sPCM was collected from the animal at d 3 after implantation. The bioluminescent bacteria were then inoculated on the sPCM and maintained under standard culture conditions in an incubator with humidified air containing 5% CO₂ at 37°C for 12 and 24 h before imaging.

RNA isolation, reverse transcription, and quantitative RT-PCR

Total RNA was isolated from wound macrophages at d 3 using a mirVana RNA Isolation Kit (Thermo Fisher Scientific). Extracted RNA was quantified using NanoDrop (Thermo Fisher Scientific), and total cDNA synthesis was achieved using the SuperScriptVilo cDNA Synthesis Kit (Thermo Fisher Scientific). mRNA was measured using SYBR Green DNA binding dye by quantitative PCR assay. 18S and β -actin were used as reference housekeeping genes. The primer sets we used are listed in Table 1.

TABLE 1. *Primer sets*

Primer	Sequence, 5'-3'
18S_F	GTAACCCGTTGAACCCCAT
18S_R	CCATCCAATCGGTAGTAGCC
mVEGF_F	GTCAGAGAGCAACATCACCATGCA
mVEGF_R	CCTTGCAACCGGAGTCTGTCTT
mTNF- α _F	TCCCAGGTTCTCTTCAAGGGA
mTNF- α _R	GGTGAGGAGCACGTAGTCCG
mIL-10_F	CTGCTATGCTGCTGCTCTT
mIL-10_R	CAGCTGGTCTTTGTTTGAA
mIL-1 β _F	AGCACCTCACAAAGCAGAGCACAA
mIL-1 β _R	CGGATTCCATGGTGAAGTCAATT
mArg-1_F	GCCGGTGGAGAGGAGCTGGA
mArg-1_R	AAAGGCCAGTCCCGCTGGT
miNOS_F	GTGACAAGCAC` ATTTGGGAATGGA
miNOS_R	CTGAGTTCGTCCTTCTCTGTT
hDEFB1-F	AGGAGCCAGCGTCTCCCCAG
hDEFB1-R	GCCCTCCACTGCTGACGCAA
hS100A9-F	CTGGGGCACCCAGACACCCT
hS100A9-R	CCTCCCCGAGGCTGGCTTA
hBactin-F	TGGTGGGCATGGGTCAGA
hBactin-R	GTACATGGCTGGGGTGTGGA
mTGF- β _F	CCGCAACAACGCCATCTATG
mTGF- β _R	TGCCGTACAACCTCCAGTGAC
mMRC1_F	GGAGGGTGGGACCTGGCAA
mMRC1_R	TCACAGGCTCTGTCCGCCCA
mCD74_F	GGCTCTGCTCTTGGCTGGGC
mCD74_R	AGCTGCGGTTACTCCAGGGG
mCD163_F	CGATGACCTGGCATGCAATG
mCD163_R	ATGGCAGTTGGACATCCCAG
mIL-12_F	GACCAGGCAGCTCGCAGCAA
mIL-12_R	CCAGGGGCATCGGGAGTCCA

Enzyme-linked immunosorbent assay

The concentration of IL-1 β , TNF- α , VEGF, and IL-10 cytokines in wound tissues (R&D Systems, Minneapolis, MN, USA) were quantified using commercially available ELISA kits as previously described (27, 28). Cytokine levels were normalized against protein concentrations measured using a bicinchoninic acid protein assay.

Flow cytometry analysis

Wound cells were isolated from polyvinyl alcohol sponges as previously described (27). The whole cell population (1×10^6) was stained with monoclonal FITC-conjugated anti-mouse F4/80 (eBioscience). Mouse IgG1 (Bio-Rad) was used to serve as the corresponding negative control. Mean fluorescence intensity was measured by excitation of fluorochrome-coated cells with a 488 nm argon laser in a C6 Accuri Flow Cytometer (Accuri Cytometers, Ann Arbor, MI, USA) and recording FITC at 530 ± 15 nm, as previously described (30). Each sample was represented by 10,000 gated cells. Data are shown as percentage of positive cells in the whole population. Background fluorescence correction was factored into the data analysis process.

Histology and immunohistochemistry

Briefly, paraffin-embedded tissues were cut into 8- μ m thick sections. After deparaffinization and hydration, sections were stained with hematoxylin and eosin. For immunostaining, sodium citrate (pH 6.0) antigen retrieval was performed, and sections were blocked with 10% normal goat serum at room temperature, then

incubated with rabbit pAb of K14 (PRB-155P-100; 1:400; Covance, Princeton, NJ, USA) overnight at 4°C. Signal was visualized by subsequent incubation with fluorescence-tagged secondary antibodies (Alexa Fluor 568-tagged α -rabbit, 1:200). Mosaic images at $\times 20$ were collected using Axioscanner (Zeiss).

Picrosirius red and Herovici staining

Formalin-fixed, paraffin-embedded specimens were sectioned. The paraffin sections were deparaffinized and stained with picrosirius red using standard procedures (31). Picrosirius red staining is used to distinguish between type I and type III collagen in wound tissues; type I (thick fibers) appears as yellow-orange birefringence, whereas type III (thin fibers) appears as green birefringence when viewed under a polarized light microscope. The Herovici Collagen Staining Kit (KATHER; American MasterTech, Lodi, CA, USA) was used to stain paraffin-embedded tissues as previously described (32). Young collagen and reticulum stain blue, mature collagen red, cytoplasm yellow, and nuclei black.

Atomic force microscopy

Atomic force microscopy (AFM) was used to characterize the mechanics of sPCM immersed in distilled water. All measurements were conducted using MFP-3D-Bio AFM (Asylum Research, Santa Barbara, CA, USA). Silicon nitride cantilevers with nominal spring constant of 0.01 N/m, length of 310 μ m, width of 20 μ m, and a 4-sided pyramidal tip (Bruker AFM Probes, Camarillo, CA, USA) were used. Using a method previously described (33), 4 regions of $50 \times 50 \mu$ m were scanned under contact mode, and a force map of 10×10 data points was captured per image. The force-displacement curves were analyzed using a commercial software (Oxford Instruments; Asylum Research, Santa Barbara, CA, USA) to measure Young's modulus (E) using a Oliver-Pharr model. All data were analyzed using a histogram distribution and are reported as relative frequency with respect to the total number of measurements collected. Information of height distribution and surface topography (deflection error) were also collected from the scanned regions.

Scanning electron microscopy

Samples were fixed with glutaraldehyde and dehydrated. Next, samples were treated with hexamethyldisilazane (Ted Pella, Redding, CA, USA) and left overnight for drying. Before scanning, samples were mounted on an aluminum stub and coated with gold/palladium. Imaging of the samples was done by using an FEI Nova nano-scanning electron microscopy (SEM) scanning electron microscope (FEI Co., Hillsboro, OR, USA) equipped with a field-emission gun electron source. Processing and imaging of samples were performed as previously described (13, 29). At least 4 regions of interest from different locations of each sample ($n = 6$) were imaged.

Statistical analyses

Data are expressed as means \pm SD of at least 4 to 6 animals per group. Significance between 2 groups was tested by a 2-tailed Student's *t* test. A value of $P < 0.05$ was considered statistically significant.

RESULTS

Structural characterization of sPCM

SEM analyses depicted structured organization of collagen fibers in the intact dressing with characteristic light and dark bands (Fig. 1A). Light microscopic images showed uneven topography of the dressing with randomly oriented collagen bundles (Fig. 1B). Stiffness measurements were conducted in wet samples. There was a significant increase in the sample volume once the sample was hydrated, and it acquired hydrogel-like material properties. The stiffness measurements were in the range of 1 to 5 MPa, which is higher than what has been reported in the literature for collagen gels, but closer to skin modulus distribution, peaking at 322 kPa and ranging from 25.8 kPa to 1.18 MPa (34) (Fig. 1C). Images of height distribution and

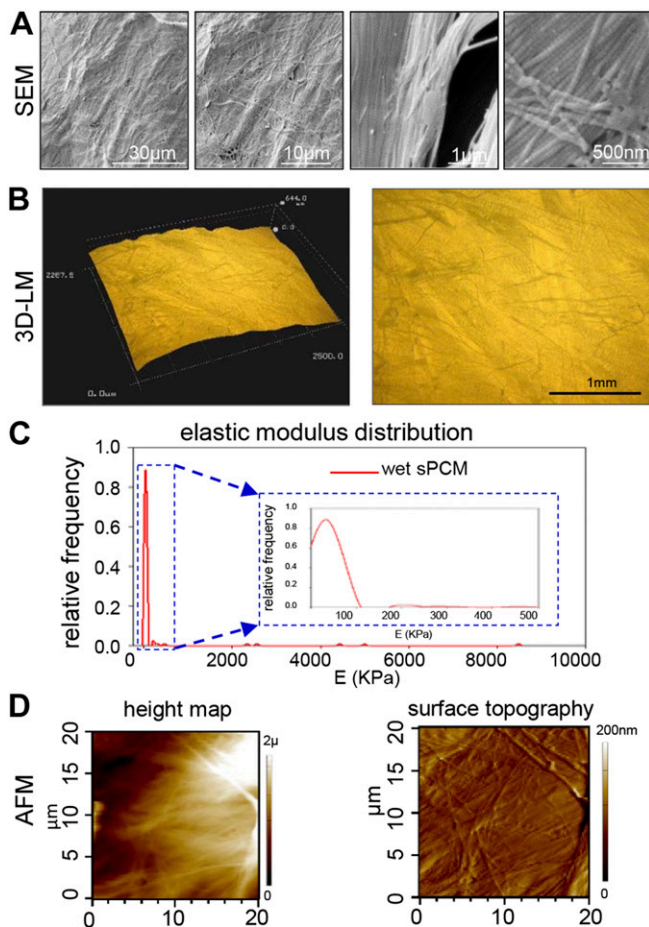


Figure 1. Advanced microscopy-based characterization of sPCM. *A)* SEM images show structured organization of collagen fibers in intact dressing with alternating light and dark bands. *B)* 3D light microscopic images show uneven topography of dressing with randomly oriented collagen bundles. Scale bar, 1 mm. *C)* AFM of sPCM immersed in deionized water. Histogram distribution of E obtained for $50 \times 50\text{-}\mu\text{m}$ regions scanned under contact mode with minimum and maximum values of 0.56 kPa and 8.52 MPa, respectively. Inset provides detail of highest frequency estimated, $E = 35.5$ KPa. *D)* Representative images of height distribution and surface topography of sPCM immersed in distilled water.

surface topography of sPCM immersed in distilled water are shown in Fig. 1D.

Wound inflammation

To test the effect of sPCM on inflammation related cells, the dressing was sandwiched in polyvinyl alcohol sponges and was implanted subcutaneously. SEM analysis of the collected sPCM showed increased macrophage recruitment at d 3 compared to control (Fig. 2A). Infiltrating cells at the wound site were collected on d 3 and 7. Flow cytometric analyses of $F4/80^+$ cells revealed significantly higher recruitment of macrophages to the wound site. However, by d 7, the count of such cells markedly dropped, indicative of rapid resolution of inflammation (Fig. 2B). Interestingly, sPCM did not influence the $Ly6C$ subpopulation of recruited $CD11b^+$ cells (Supplemental Fig. S5).

Efferocytosis

A significantly increased efferocytosis index was noted in macrophages collected from sPCM-treated wound fluids compared to untreated controls (Fig. 3 and Supplemental Fig. S2).

Macrophage cytokine markers

Infiltrating wound site macrophages were isolated using $CD11b$ magnetic bead separation and subjected to real-time quantitative PCR analyses. During the early inflammatory phase (d 3), sPCM markedly induced proinflammatory markers such as $IL-1\beta$, $iNOS$, and $TNF-\alpha$ (Fig. 4A and Supplemental Fig. S4A). At this early time point, cells exposed to sPCM were ready to mount resolution of inflammation, as indicated by elevated levels of proresolution genes such as $IL-10$, $arginase-1$, and $VEGF$ (Fig. 4B and Supplemental Fig. S4B). On d 7, sPCM significantly attenuated proinflammatory markers $IL-1\beta$, $IL-12$, and $CD74$ while up-regulating the levels of proresolution genes such as $arginase-1$ and $VEGF$ and $TGF-\beta$ (Fig. 4C, D and Supplemental Fig. S4C, D). Consistent data were obtained from excisional wound studies. Analysis of cytokines of wound-edge tissue from such studies on d 7 and 14 after wounding showed lowering of the proinflammatory cytokines $IL-1\beta$ and $TNF-\alpha$. In these samples, proresolution $IL-10$ and $VEGF$ were up-regulated, indicative of rapid and efficient resolution of inflammation (Fig. 5).

Antimicrobial peptides

To characterize the role of sPCM in host defenses, human HaCaT keratinocytes were grown on sPCM for 24 h. Cells exposed to sPCM exhibited a differentiating phenotype as differentiating cells assemble

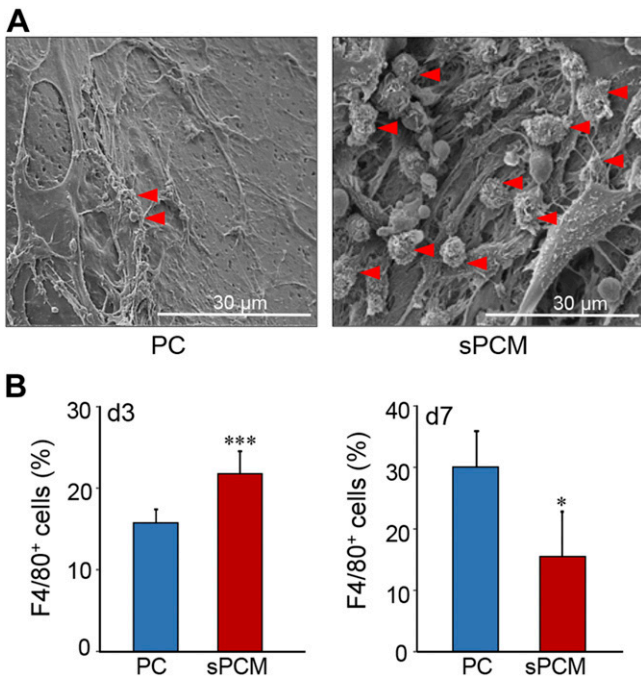


Figure 2. Macrophage recruitment. *A*) Representative SEM images of collected sPCM d 3 after implantation, showing more macrophage recruitment compared to PC. Macrophage is marked with red arrowhead. *B*) Graphical representation of macrophage (F4/80 is macrophage marker) content in collected sPCM at d 3 and 7, as evident from flow cytometry analysis. Data are presented as means \pm SD. *** $P < 0.001$ ($n = 6$), * $P < 0.05$ ($n = 4$).

desmosomal and adherens junctions (35) (Fig. 6A). The differentiating keratinocytes are known to acquire specialized antimicrobial resistance (36, 37). Consistently, keratinocytes exposed to sPCM exhibited induction of antimicrobial proteins S100A9 and β -defensin-1 (Fig. 6B).

Inhibition of biofilm formation

Adherence of *Pseudomonas aeruginosa* (PA01) on sPCM pre-exposed to host immune cells *in vivo* was inhibited (Fig. 7A and Supplemental Fig. S3). Inhibition of biofilm formation was evident by IVIS imaging using bioluminescent strains of *P. aeruginosa* (Xen41) and *S. aureus* (SAP231). Bacterial proliferation and metabolic activity were significantly decreased in sPCM primed with host exposure (Fig. 7B, C).

Wound re-epithelialization

Excisional wounds dressed with sPCM showed complete closure at d 14 compared to the Tegaderm-dressed control wounds (Fig. 8A). Histologic analyses using hematoxylin and eosin staining showed complete re-epithelialization (Fig. 8B). Significant decrease in wound area was observed in sPCM-treated mice at d 14 compared to the Tegaderm-dressed control wounds (Fig. 8C). Finally, K14 staining showed

complete re-epithelialization of sPCM dressed wounds, while Tegaderm-dressed wounds remained open (Fig. 9).

Wound tissue collagen

sPCM dressing of excisional wounds resulted in repaired skin with a higher abundance of mature collagen deposition, as evident by picrosirius red stain. Higher collagen I:III ratio (yellow-orange fibers to green fibers) was noted in sPCM-treated wounds compared to those dressed with Tegaderm (Fig. 10A). Consistent findings were obtained using Herovici staining, which revealed that sPCM dressing increased mature collagen content (red fibers) with higher collagen I:III ratio in d 14 samples after wounding (Fig. 10B).

DISCUSSION

sPCM is an equine pericardium that is decellularized, stabilized (cross-linking), and sterilized with ethylene dichloride to preserve the native structure of collagen. This process results in a fully flexible cross-linked tissue that is resistant to proteolytic enzyme degradation (24). The triple helix of the collagen molecule is resistant to most

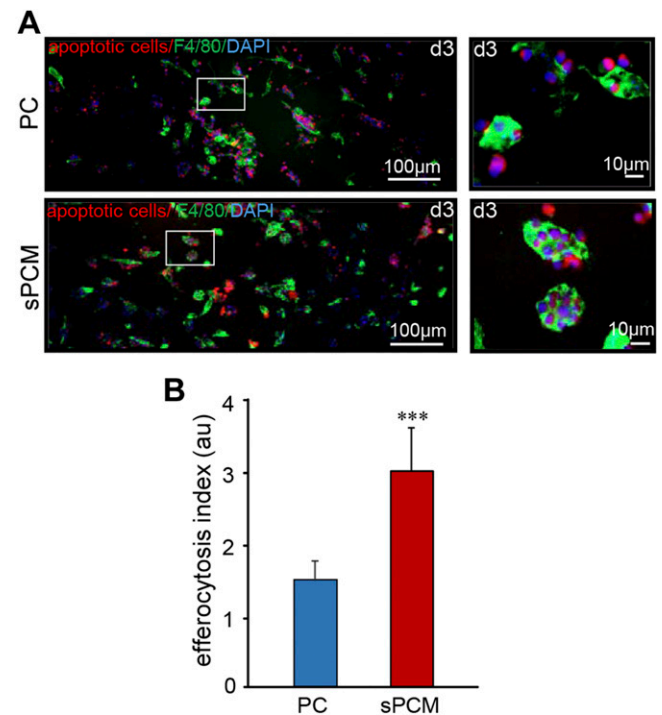


Figure 3. sPCM supports efferocytosis and resolves inflammation at wound site. *A*) Representative images of wound macrophages collected from C57BL/6 mice (F4/80, green) cocultured with apoptotic cells (pHrodo, red). Inset: images showing single macrophage with engulfed apoptotic cells (scale bar, 10 μ m). *B*) Efferocytosis index of d 3 wound macrophage. Efferocytosis index is defined as total number of engulfed apoptotic cells per macrophage present in field of view. Data are presented as means \pm SD. *** $P < 0.001$ ($n = 3$).

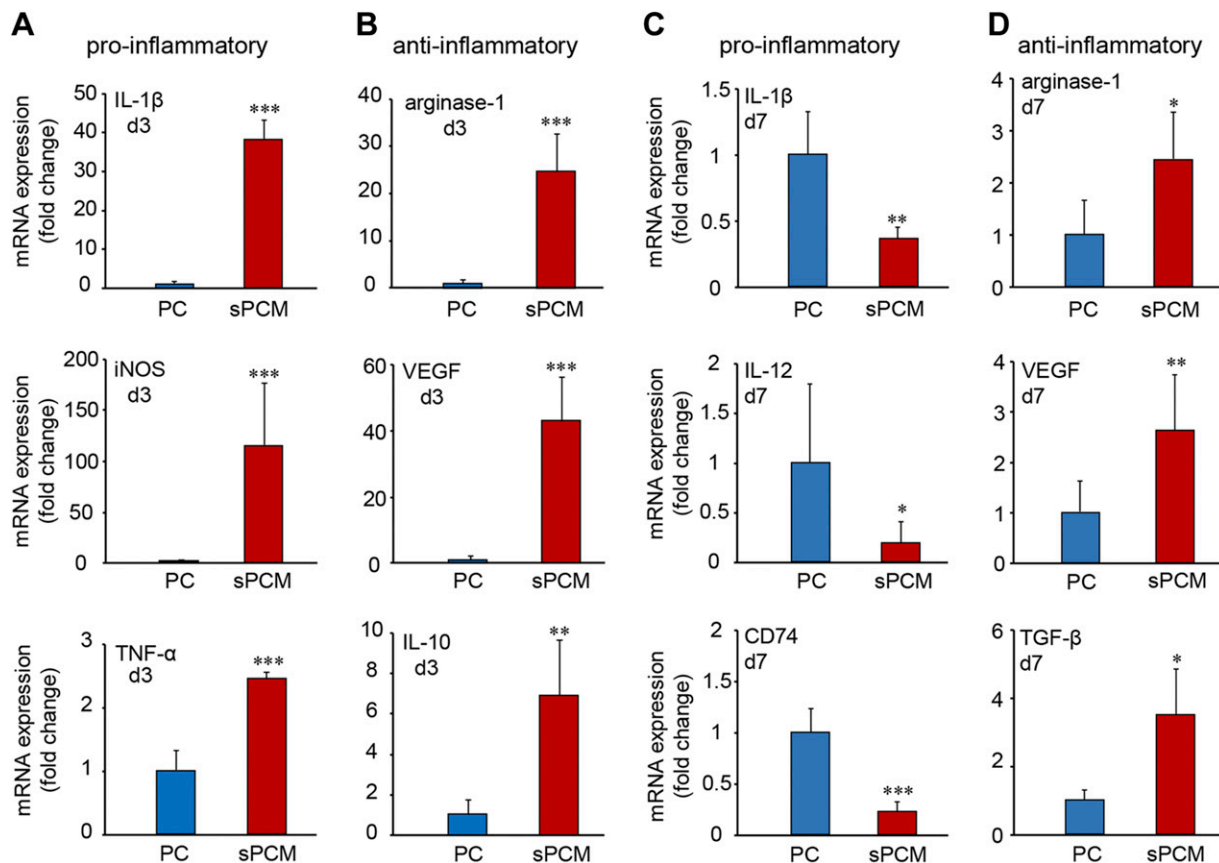


Figure 4. sPCM promoted up-regulation of pro- and anti-inflammatory markers from wound inflammatory cells. Expression of proinflammatory markers at d 3 and 7 (A, C) and anti-inflammatory markers (B, D) were measured using quantitative PCR from d 3 isolated macrophages collected from sPCM postimplantation subcutaneously. Data are presented as means \pm SD. * $P < 0.05$, ** $P < 0.01$, *** $P < 0.001$ ($n = 4$).

proteases, which are affected by the collagen fibril architecture that is resistant to proteolysis (38). The characteristic band pattern of light and dark regions observed in SEM analyses of sPCM is consistent with the banding structure of collagen fibers (39, 40). Light microscopic images of sPCM show uneven topography of the dressing with randomly oriented collagen bundles. These fibrils are stabilized by covalent cross-linking of specific lysines and hydroxylsines of the collagen molecules, which are ordered parallel in a D-periodic pattern (41). Mechanical properties of the wound surface defend against shearing forces and external trauma. sPCM stiffness was detected to be in the range of 1 to 5 mPa. Unlike that of other collagen gels, such stiffness is closer to skin modulus distribution (34). Also analogous to the normal healthy skin is the height map and surface topography of the hydrated sPCM (34, 42). Taken together, sPCM exhibited unique characteristics that were not comparable to collagen gel dressings but were more closely aligned to properties of the healthy skin.

Robust mounting of an inflammatory response followed by timely resolution of inflammation is critical for successful wound healing (31). Macrophages with complex subpopulation play a pivotal role in the inflammatory cascade. Given the current ambiguity in macrophage nomenclature specifically for tissue macrophages (43, 44), and proposed misfit of wound

macrophage with the M1/M2 nomenclature (45–47), for this work, we classify *in vivo* wound macrophages on the basis of the proinflammatory or proresolution/healing polarization states. Failure to mount robust wound inflammation is recognized as a significant limitation in several clinical conditions (48–50). It is evident from this work that sPCM elicits signals that can successfully recruit macrophages to the site of the injury. Such observation is consistent with previous finding from our laboratory reporting the ability of collagen-based dressings to increase recruitment of macrophages to the wound site (27, 31). Macrophages thus recruited to the wound site by sPCM were not only higher in abundance but also functionally more effective, as evidenced by their cytokine response and efferocytosis index. Proinflammatory cytokines delivered to the wound site at an early phase prepares the wound for the healing process (51, 52). sPCM was clearly effective in achieving such delivery. Synchronous with proinflammatory cytokine delivery during the early phase of wound healing, macrophages are charged with the responsibility to clean up dead or dying cells at the wound site by efferocytosis. Successful execution of such cellular debridement, as has been reported in our earlier work (27), advances the healing process. Application of sPCM dressing to the wound site markedly enhanced the ability of each

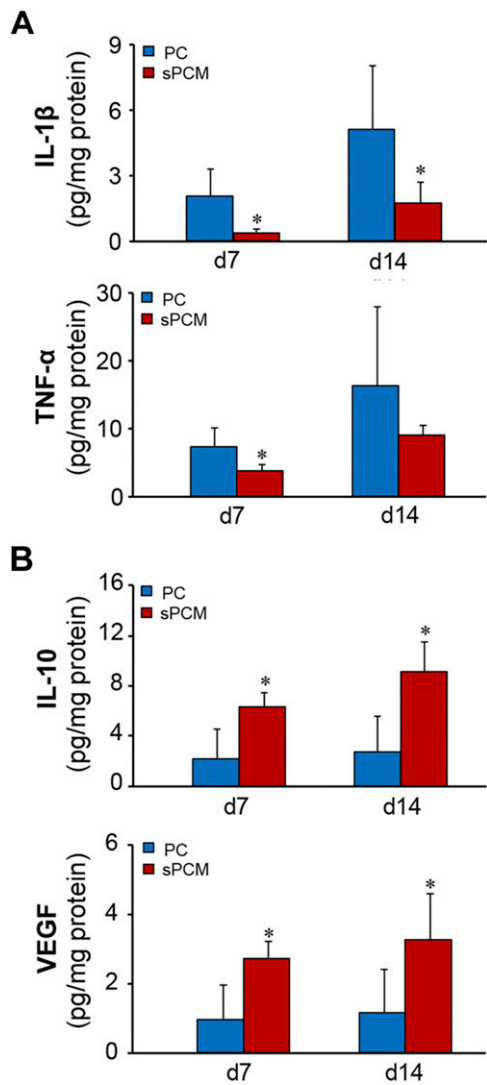


Figure 5. sPCM promoted rapid resolution of inflammation. Expression of proinflammatory markers from collected tissues at d 7 and 14 (A) and anti-inflammatory markers at d 7 and 14 (B) were measured using ELISA from collected mice wound tissues. Data are presented as means \pm SD. * $P < 0.05$ ($n = 5$).

wound macrophage to cleanse the wound microenvironment. At the site of injury, monocytes and macrophages may be also studied as Ly6C^{hi} or Ly6C^{lo} subsets (53–55). The significance of this marker under *ex vivo* and *in vivo* conditions may not be the same (43). This binary classification does not seem to address the more complex heterogeneity of these cells *in vivo*, where macrophages adopt distinct phenotypes and even switch between phenotypes in response to the myriad of stimuli to which they are exposed (44). It is proposed that Ly6C represents a macrophage differentiation marker rather than as a specific M1/M2 marker (56). Microarray profiling of the Ly-6C^{lo} subset, compared with Ly-6C^{hi} macrophages, showed a phenotype outside the M1/M2 classification (57). Although the sPCM induced clear changes in the macrophage polarization, the Ly6C subpopulations remained. Such finding suggests the lack of a direct link between the state of

macrophage polarization and Ly6C expression under *in vivo* conditions. Some of the study of wound site monocyte/macrophages relies on isolation of such cells from wound tissue employing enzymatic digestion (54). Such enzymatic tissue disintegration is likely to influence the abundance of a variety of cell-surface molecules commonly used for phenotypic analysis (58). The approach adopted in this work does not rely on enzymatic digestion of wound tissue and should be accounted for during comparative data interpretation.

Although inflammation is a critical driver of the wound healing process, its failure to resolve in a timely manner represents one of the leading causes of chronic wounds and secondary infection (31, 59). Thus, while the ability of sPCM to maximize wound inflammation is encouraging, it is of critical interest to understand its impact on the resolution of inflammation. Of interest in this context is the observation that the proresolution process in sPCM treated wounds was initiated early on d 3, making the process of inflammation robust, but sharp and transient at the same time. Therefore, on d 7, fewer macrophages were evident at the wound site after sPCM treatment. Resolution of inflammation is an active process that is achieved by a progressive shift of proinflammatory to proresolution function of the wound site macrophage population. Early and sustained

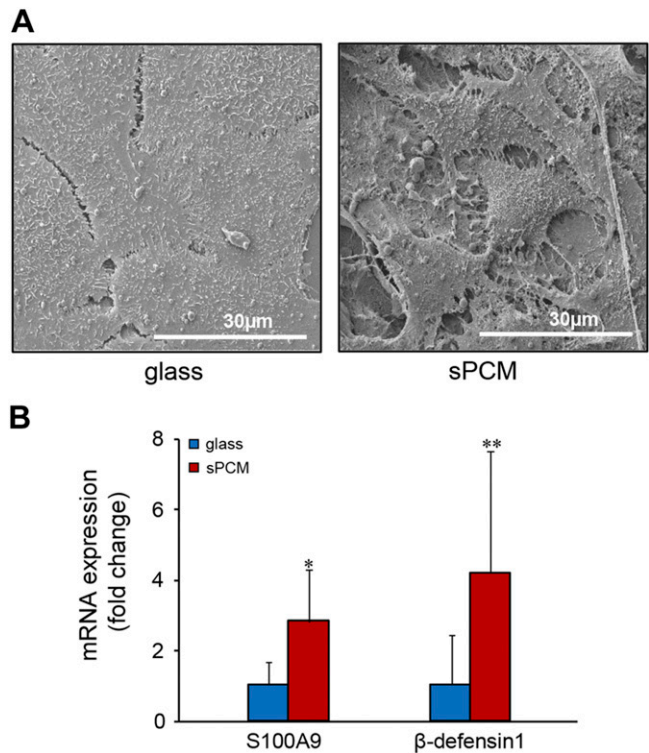


Figure 6. sPCM bolstered host immune defenses. A) Representative SEM images of HaCaT cells grown on control surface (glass coverslip) and on sPCM showing distinct morphologic differences. B) HaCaT cells grown on sPCM for 24 h showed up-regulation of AMPs-S100A9 and β -defensin-1. Gene expression data are presented as fold change. Data are presented as means \pm SD. * $P < 0.05$, ** $P < 0.01$ ($n = 5$).

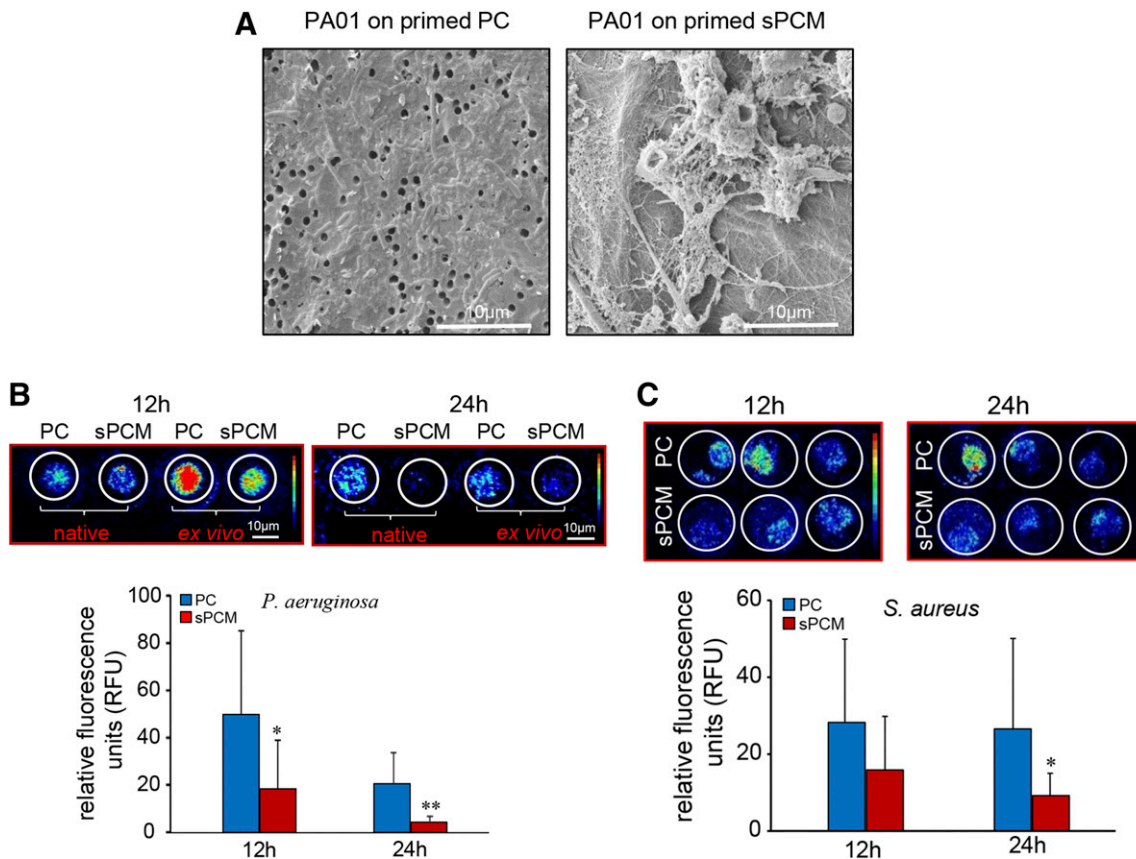


Figure 7. Biofilm formation was inhibited on sPCM pre-exposed to host immune cells. *A*) Representative SEM images showing adherence of *P. aeruginosa* (PA01) on host immune cell primed sPCM compared to PC exposed to same conditions. *B*) Representative IVIS images of *P. aeruginosa* (Xen41; base strain PA01), taken at 12 and 24 h, showing less bacterial metabolic activity (red color, more active; blue color, less active) in sPCM compared to PC. *C*) Representative IVIS images of and *S. aureus* (SAP231; base strain USA300) taken at 12 and 24 h showing less bacterial metabolic activity in sPCM compared to PC. Average intensity of bacterial activity was quantified and plotted. Data are presented as means \pm sd. * $P < 0.05$, ** $P < 0.01$ ($n = 5$).

up-regulation of anti-inflammatory cytokines such as IL-10 and VEGF in response to sPCM represent a major mechanism supporting early wound closure (60–63). VEGF, induced in wound-edge keratinocytes and macrophages, promotes healing through increased angiogenesis (64). Proresolution macrophages produce copious amount of IL-10, which advances the healing cascade (65–67). Such modulation of the wound microenvironment by sPCM made the inflammatory process transient, thus preparing the wound for closure. Rapid re-epithelialization and early closure of the wounds were achieved by the use of sPCM as a dressing.

Open wounds readily lend themselves to pathogenic microbial colonization, especially under conditions of diabetes and other such clinical conditions, thus limiting the antimicrobial properties of the wound tissue. Under such conditions of limited host defense, microbial colonization is known to lead to biofilm infection of the wound (13, 68, 69). The Centers for Disease Control and Prevention estimates that 65% of all human infections are caused by bacteria with a biofilm phenotype, and the U.S. National Institutes of Health estimates that this number is closer to 80% (70). Of host innate immune

defenses, defensins are family members of antimicrobial peptides (AMPs) expressed by keratinocytes and mucosal epithelial cells (69, 71, 72). AMPs are known to possess antibacterial, antifungal, and antiviral activity (73, 74). Although several mechanistic models have been proposed to explain the role of AMPs *in vitro*, the search for a validated model that account for their function in tissue injury *in vivo* remains open (75–77). Human β -defensin-1 (HBD-1) is an atypical chemokine that has a chemokine-like function. Although structurally compared to other chemokines, HBD-1 may activate chemokine receptors (*e.g.*, CCR6, the receptor for CCL20) and mediates chemotactic responses for immature dendritic cells and memory T cells (74, 78–80). The expression and regulation of HBDs highlight the functional importance of each HBD in skin immunity. β -Defensin, for example, exhibits activity against the common skin pathogens *S. aureus* and *P. aeruginosa* (81). *P. aeruginosa* is a well-known biofilm producer that is directly implicated in both acute and chronic infections (82). AMPs, as multifunctional peptides, directly kill microbes, and they also do so through multiple indirect mechanisms such as disruption of lipid bilayers (75). In general, cationic AMPs are driven

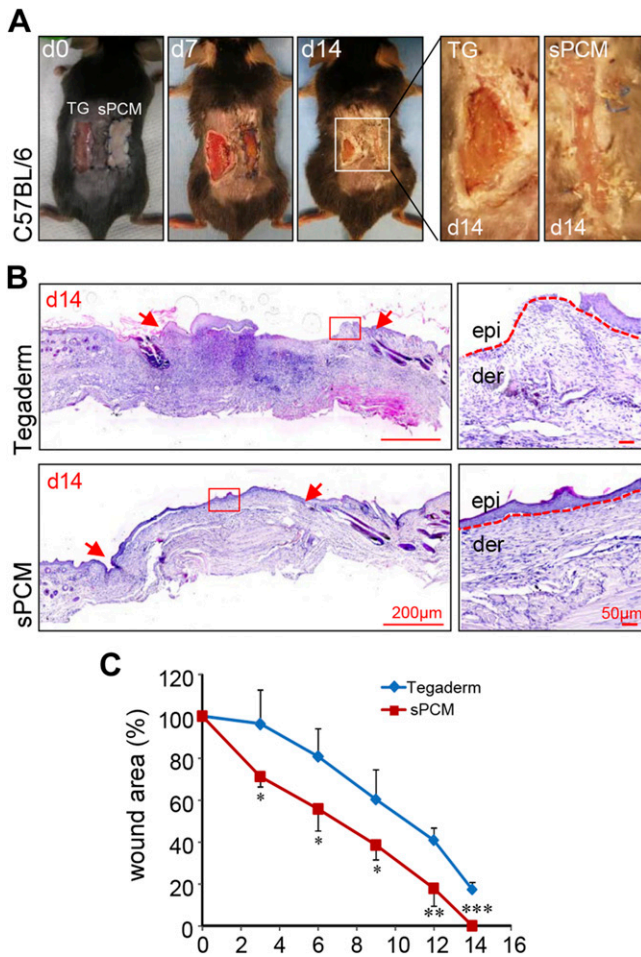


Figure 8. sPCM accelerated wound closure. *A*) Digital images of C57BL/6 mice at d 0, 7, and 14, showing complete closure of wound at d 14 in sPCM (right) compared to Tegaderm-dressed control (left). *B*) Representative hematoxylin and eosin-stained images showing full epithelialization and closure of sPCM treated wound at d 14. Wound edges are indicated by red arrows in left panel. Dermis (der) and epidermis (epi) are indicated in magnified images on the right by red dotted lines. *C*) Plotted graph of wound area percentage over time. Data are presented as means \pm SD. * $P < 0.05$, ** $P < 0.01$, *** $P < 0.001$ ($n = 4$).

by electrostatic forces to the negative phospholipid head groups on the membrane surface provided by capsular polysaccharides. Such polysaccharides include LPS in Gram-negative bacteria and teichoic acids, lipoteichoic acids, and lysylphosphatidylglycerol in Gram-positive bacteria. AMPs drill physical pores on the cell membrane, causing leakage of cytosolic content (75). Deficiency of β -defensin-1 in mice causes delayed clearance and increased colonization of pathogens in host tissue (83, 84). sPCM up-regulated human keratinocyte β -defensin as well as S100A9. S100A9 is a calgranulin with antimicrobial properties. It supports innate and acquired immune responses by promoting intra- and extracellular growth inhibition of a broad range of bacteria and fungi, as well as by bolstering leukocyte recruitment to site of injury (85, 86). This, taken together with the observation that sPCM augments recruitment of macrophages to the wound site, leads to the notion that AMP induction and recruitment of phagocytic cells represent two major related

mechanisms of action by which sPCM may prevent wound infection.

Recidivism or recurrence is a major threat in wound care (87–89). Quality of the repaired skin is therefore of paramount importance (15, 90). The state of maturation of collagen in the repaired skin is a critical determinant of its biomechanical properties (91, 92). Activated macrophages cause fibroblasts to differentiate into myofibroblasts. Myofibroblasts are characterized by their expression of α smooth muscle actin and production of collagen I, which will increase the wound tensile strength over time (64, 93). Abundant mature collagen fibers were identified in sPCM-dressed wounds. Importantly, collagen type I dominated over collagen type III. Such increased collagen type I:III ratio is crucial for appropriate wound tensile strength to support the growth of vascularized granulation tissue and to prevent dehiscence (94, 95).

In summary, the naturally derived biomaterial sPCM is a single-application collagen-based wound dressing that is capable of presenting scaffold functionality during the course of wound healing. In addition to inducing endogenous antimicrobial defense systems, the dressing itself has properties that minimize biofilm formation. It mounts robust inflammation, a process that rapidly resolves, making way for wound healing to advance. Improved wound closure was evident by accelerated epithelialization of

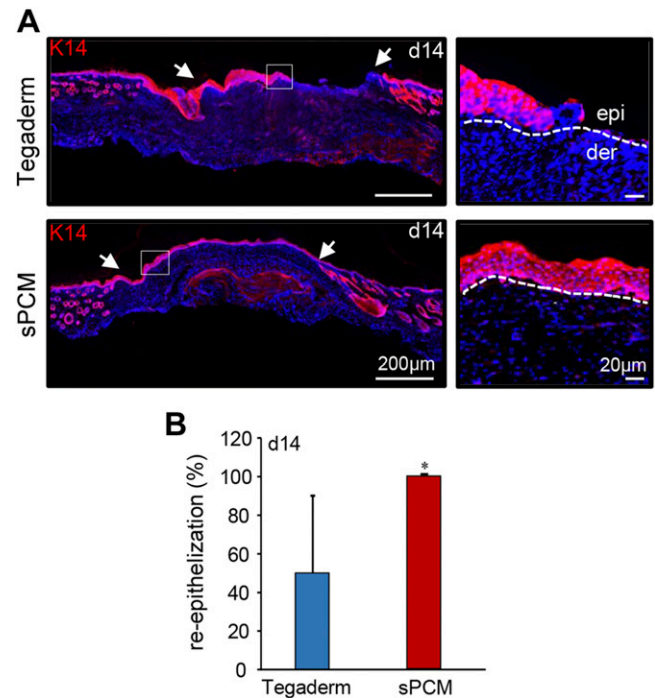


Figure 9. sPCM accelerated wound re-epithelialization. *A*) Representative images from formalin-fixed, paraffin-embedded wound tissue biopsy sections at d 14 showing immunostaining with K14. sPCM-treated wounds showed complete re-epithelialization with organization of epithelial layer. Wound edge is indicated by white arrows in left panel. Dermis is indicated by white dotted line in right panel. *B*) Significantly increased expression of K14 in sPCM compared to Tegaderm-treated wounds was observed and is represented graphically. Data are presented as means \pm SD. * $P < 0.05$ ($n = 4$).

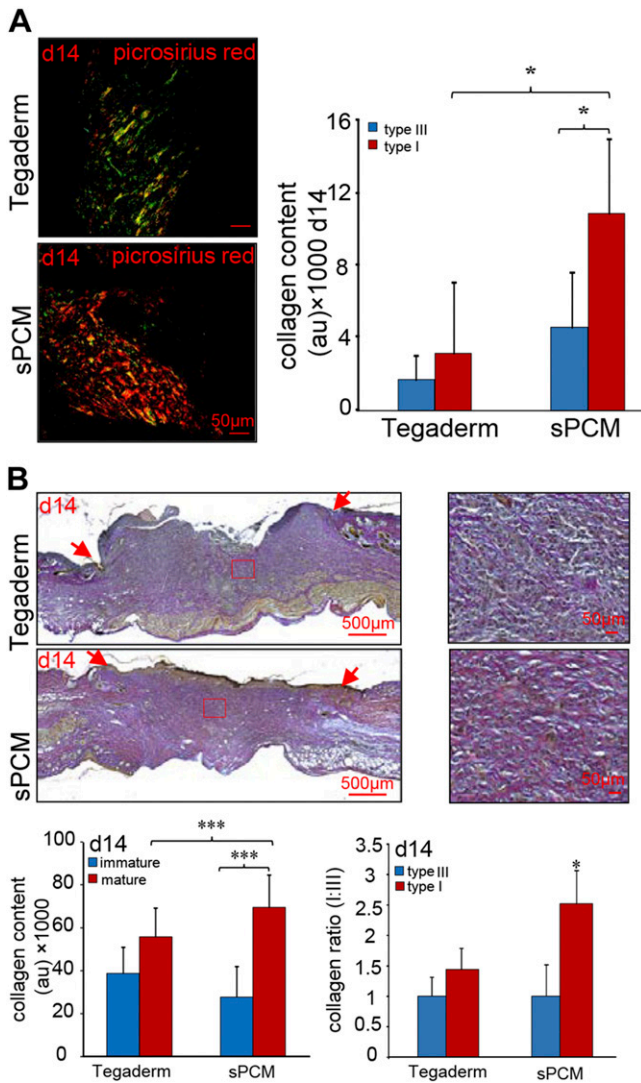


Figure 10. sPCM enhanced collagen maturation. A) Representative images from formalin-fixed, paraffin-embedded wound tissue biopsy sections at d 14 stained using picosirius red staining (PRS) showed marked increase of collagen I:III ratio (yellow-orange fibers to green fibers) in sPCM-treated wounds compared to Tegaderm-treated wounds. Collagen content was quantitated and is represented graphically (AU). Data are presented as means \pm SD. * $P < 0.05$ ($n = 4$). B) Herovici-stained wound tissue showed increased percentage of mature collagen content (mature collagen red fibers to immature blue fibers) in sPCM-treated wounds compared to Tegaderm-treated wounds at d 14 with marked increase of collagen I:III ratio. Wound edge is indicated by red arrows. Collagen content was quantitated and is represented graphically. Data are presented as means \pm SD. *** $P < 0.001$ ($n = 6$).

excisional wounds. sPCM not only expedited wound closure but also improved the quality of healing by increased collagen deposition and maturation. Randomized clinical trial testing this promising dressing material in a clinical setting is warranted. **[E]**

ACKNOWLEDGMENTS

The authors thank Dr. B. Deng (Center for Electron Microscopy and Analysis College of Engineering, The Ohio State University) for her assistance with light microscopy studies

on sPCM. This work was supported by U.S. National Institutes of Health Grants GM077185 and GM069589 (National Institute of General Medical Sciences), NR013898 and NR015676 (National Institute of Nursing Research), and DK076566 (National Institute of Diabetes and Digestive and Kidney Diseases). This work was supported, in part, by an unrestricted gift from Harbor MedTech (Irvine, CA, USA). The authors declare no conflicts of interest.

AUTHOR CONTRIBUTIONS

M. S. El Masry, S. S. Mathew-Steiner, S. Roy, R. A. Anani, and C. K. Sen designed research; M. S. El Masry, S. Chaffee, P. Das Ghatak, S. S. Mathew-Steiner, A. Das, and N. Higuaita-Castro performed research and analyzed data; and M. S. El Masry, S. Chaffee, S. S. Mathew-Steiner, A. Das, S. Roy, R. A. Anani, and C. K. Sen wrote the manuscript.

REFERENCES

- Broughton II, G., Janis, J. E., and Attinger, C. E. (2006) A brief history of wound care. *Plast. Reconstr. Surg.* **117**(7 Suppl), 6S–11S
- Shah, J. B. (2011) The history of wound care. *J. Am. Col. Certif. Wound Spec.* **3**, 65–66
- Moore, Z. (1997) Wound care: module 2. Part 1: history of wound management. *World J. Nurs.* **5**, 15–16
- Lebeaux, D., Ghigo, J. M., and Beloin, C. (2014) Biofilm-related infections: bridging the gap between clinical management and fundamental aspects of recalcitrance toward antibiotics. *Microbiol. Mol. Biol. Rev.* **78**, 510–543
- Rubin, R. H. (2006) Surgical wound infection: epidemiology, pathogenesis, diagnosis and management. *BMC Infect. Dis.* **6**, 171
- Dhivya, S., Padma, V. V., and Santhini, E. (2015) Wound dressings—a review. *Biomedicine (Taipei)* **5**, 22
- Boateng, J. S., Matthews, K. H., Stevens, H. N., and Eccleston, G. M. (2008) Wound healing dressings and drug delivery systems: a review. *J. Pharm. Sci.* **97**, 2892–2923
- Ramos-e-Silva, M., and Ribeiro de Castro, M. C. (2002) New dressings, including tissue-engineered living skin. *Clin. Dermatol.* **20**, 715–723
- Srecker-McGraw, M. K., Jones, T. R., and Baer, D. G. (2007) Soft tissue wounds and principles of healing. *Emerg. Med. Clin. North Am.* **25**, 1–22
- Yazdanpanah, L., Nasiri, M., and Adarvishi, S. (2015) Literature review on the management of diabetic foot ulcer. *World J. Diabetes* **6**, 37–53
- Barki, K. G., Das, A., Dixith, S., Ghatak, P. D., Mathew-Steiner, S., Schwab, E., Khanna, S., Wozniak, D. J., Roy, S., and Sen, C. K. (2017) Electric field based dressing disrupts mixed-species bacterial biofilm infection and restores functional wound healing. [E-pub ahead of print] *Ann. Surg.* DOI: 10.1097/SLA.0000000000002504
- Kirschner, N., Rosenthal, R., Günzel, D., Moll, I., and Brandner, J. M. (2012) Tight junctions and differentiation—a chicken or the egg question? *Exp. Dermatol.* **21**, 171–175
- Roy, S., Elgharably, H., Sinha, M., Ganesh, K., Chaney, S., Mann, E., Miller, C., Khanna, S., Bergdall, V. K., Powell, H. M., Cook, C. H., Gordillo, G. M., Wozniak, D. J., and Sen, C. K. (2014) Mixed-species biofilm compromises wound healing by disrupting epidermal barrier function. *J. Pathol.* **233**, 331–343
- Ghatak, S., Chan, Y. C., Khanna, S., Banerjee, J., Weist, J., Roy, S., and Sen, C. K. (2015) Barrier function of the repaired skin is disrupted following arrest of dicer in keratinocytes. *Mol. Ther.* **23**, 1201–1210
- Xue, M., and Jackson, C. J. (2015) Extracellular matrix reorganization during wound healing and its impact on abnormal scarring. *Adv. Wound Care (New Rochelle)* **4**, 119–136
- Jayakumar, R., Prabakaran, M., Sudheesh Kumar, P. T., Nair, S. V., and Tamura, H. (2011) Biomaterials based on chitin and chitosan in wound dressing applications. *Biotechnol. Adv.* **29**, 322–337
- Sheridan, R. L., and Moreno, C. (2001) Skin substitutes in burns. *Burns* **27**, 92
- Fleck, C. A., and Chakravarthy, D. (2007) Understanding the mechanisms of collagen dressings. *Adv. Skin Wound Care* **20**, 256–259
- Seif-Naraghi, S. B., Salvatore, M. A., Schup-Magoffin, P. J., Hu, D. P., and Christman, K. L. (2010) Design and characterization of an

- injectable pericardial matrix gel: a potentially autologous scaffold for cardiac tissue engineering. *Tissue Eng. Part A* **16**, 2017–2027
20. Badylak, S. F., and Gilbert, T. W. (2008) Immune response to biologic scaffold materials. *Semin. Immunol.* **20**, 109–116
 21. Zheng, M. H., Chen, J., Kirilak, Y., Willers, C., Xu, J., and Wood, D. (2005) Porcine small intestine submucosa (SIS) is not an acellular collagenous matrix and contains porcine DNA: possible implications in human implantation. *J. Biomed. Mater. Res. B Appl. Biomater.* **73**, 61–67
 22. Fleischli, J. G., Laughlin, T. J., and Fleischli, J. W. (2009) Equine pericardium collagen wound dressing in the treatment of the neuropathic diabetic foot wound: a pilot study. *J. Am. Podiatr. Med. Assoc.* **99**, 301–305
 23. Mulder, G., and Lee, D. K. (2009) A retrospective clinical review of extracellular matrices for tissue reconstruction: equine pericardium as a biological covering to assist with wound closure. *Wounds* **21**, 254–261
 24. Nataraj, C., Ritter, G., Dumas, S., Helfer, F. D., Brunelle, J., and Sander, T. W. (2007) Extracellular wound matrices: novel stabilization and sterilization method for collagen-based biologic wound dressings. *Wounds* **19**, 148–156
 25. Alexander, J. H., Yeager, D. A., Stern, D. S., Messina, C. A., Griffith, B. J., Pacocha, E., and Barakat, M. (2012) Equine pericardium as a biological covering for the treatment of diabetic foot wounds: a prospective study. *J. Am. Podiatr. Med. Assoc.* **102**, 352–358
 26. Zelen, C. M., Gould, L., Serena, T. E., Carter, M. J., Keller, J., and Li, W. W. (2015) A prospective, randomized, controlled, multi-centre comparative effectiveness study of healing using dehydrated human amnion/chorion membrane allograft, bioengineered skin substitute or standard of care for treatment of chronic lower extremity diabetic ulcers. *Int. Wound J.* **12**, 724–732
 27. Das, A., Ghatak, S., Sinha, M., Chaffee, S., Ahmed, N. S., Parinandi, N. L., Wohleb, E. S., Sheridan, J. F., Sen, C. K., and Roy, S. (2016) Correction of MFG-E8 resolves inflammation and promotes cutaneous wound healing in diabetes. *J. Immunol.* **196**, 5089–5100
 28. Khanna, S., Biswas, S., Shang, Y., Collard, E., Azad, A., Kauh, C., Bhasker, V., Gordillo, G. M., Sen, C. K., and Roy, S. (2010) Macrophage dysfunction impairs resolution of inflammation in the wounds of diabetic mice. *PLoS One* **5**, e9539
 29. Barki, K. G., Das, A., Dixith, S., Ghatak, P. D., Mathew-Steiner, S., Schwab, E., Khanna, S., Wozniak, D. J., Roy, S., and Sen, C. K. (2017) Electric field based dressing disrupts mixed-species bacterial biofilm infection and restores functional wound healing. [E-pub ahead of print] *Ann. Surg.* 10.1097/SLA.0000000000002504
 30. Awad, H., Abas, M., Elgharably, H., Tripathi, R., Theofilos, T., Bhandary, S., Sai-Sudhakar, C., Sen, C. K., and Roy, S. (2012) Endogenous opioids in wound-site neutrophils of sternotomy patients. *PLoS One* **7**, e47569
 31. Elgharably, H., Ganesh, K., Dickerson, J., Khanna, S., Abas, M., Ghatak, P. D., Dixit, S., Bergdall, V., Roy, S., and Sen, C. K. (2014) A modified collagen gel dressing promotes angiogenesis in a preclinical swine model of chronic ischemic wounds. *Wound Repair Regen.* **22**, 720–729
 32. Sebastian, A., Syed, F., Perry, D., Balamurugan, V., Colthurst, J., Chaudhry, I. H., and Bayat, A. (2011) Acceleration of cutaneous healing by electrical stimulation: degenerate electrical waveform down-regulates inflammation, up-regulates angiogenesis and advances remodeling in temporal punch biopsies in a human volunteer study. *Wound Repair Regen.* **19**, 693–708
 33. Higuera-Castro, N., Mihai, C., Hansford, D. J., and Ghadiali, S. N. (2014) Influence of airway wall compliance on epithelial cell injury and adhesion during interfacial flows. *J. Appl. Physiol.* **117**, 1231–1242
 34. Grant, C. A., Twigg, P. C., and Tobin, D. J. (2012) Static and dynamic nanomechanical properties of human skin tissue using atomic force microscopy: effect of scarring in the upper dermis. *Acta Biomater.* **8**, 4123–4129
 35. Gniadecki, R., Olszewska, H., and Gajkowska, B. (2001) Changes in the ultrastructure of cytoskeleton and nuclear matrix during HaCaT keratinocyte differentiation. *Exp. Dermatol.* **10**, 71–79
 36. Oren, A., Ganz, T., Liu, L., and Meerloo, T. (2003) In human epidermis, beta-defensin 2 is packaged in lamellar bodies. *Exp. Mol. Pathol.* **74**, 180–182
 37. Braff, M. H., Di Nardo, A., and Gallo, R. L. (2005) Keratinocytes store the antimicrobial peptide cathelicidin in lamellar bodies. *J. Invest. Dermatol.* **124**, 394–400
 38. Perumal, S., Antipova, O., and Orgel, J. P. (2008) Collagen fibril architecture, domain organization, and triple-helical conformation govern its proteolysis. *Proc. Natl. Acad. Sci. USA* **105**, 2824–2829
 39. Williams, B. R., Gelman, R. A., Poppke, D. C., and Piez, K. A. (1978) Collagen fibril formation. Optimal *in vitro* conditions and preliminary kinetic results. *J. Biol. Chem.* **253**, 6578–6585
 40. Strasser, S., Zink, A., Janko, M., Heckl, W. M., and Thalhammer, S. (2007) Structural investigations on native collagen type I fibrils using AFM. *Biochem. Biophys. Res. Commun.* **354**, 27–32
 41. Kadler, K. E., Holmes, D. F., Trotter, J. A., and Chapman, J. A. (1996) Collagen fibril formation. *Biochem. J.* **316**, 1–11
 42. Achterberg, V. F., Buscemi, L., Diekmann, H., Smith-Clerc, J., Schwengler, H., Meister, J. J., Wenck, H., Gallinat, S., and Hinz, B. (2014) The nano-scale mechanical properties of the extracellular matrix regulate dermal fibroblast function. *J. Invest. Dermatol.* **134**, 1862–1872
 43. Murray, P. J., Allen, J. E., Biswas, S. K., Fisher, E. A., Gilroy, D. W., Goerdt, S., Gordon, S., Hamilton, J. A., Ivashkiv, L. B., Lawrence, T., Locati, M., Mantovani, A., Martinez, F. O., Mege, J. L., Mosser, D. M., Natoli, G., Saeij, J. P., Schultze, J. L., Shirey, K. A., Sica, A., Suttles, J., Udalova, I., van Genderachter, J. A., Vogel, S. N., and Wynn, T. A. (2014) Macrophage activation and polarization: nomenclature and experimental guidelines. *Immunity* **41**, 14–20
 44. Mosser, D. M., and Edwards, J. P. (2008) Exploring the full spectrum of macrophage activation. *Nat. Rev. Immunol.* **8**, 958–969; erratum: **10**, 460
 45. Das, A., Sinha, M., Datta, S., Abas, M., Chaffee, S., Sen, C. K., and Roy, S. (2015) Monocyte and macrophage plasticity in tissue repair and regeneration. *Am. J. Pathol.* **185**, 2596–2606
 46. Brancato, S. K., and Albina, J. E. (2011) Wound macrophages as key regulators of repair: origin, phenotype, and function. *Am. J. Pathol.* **178**, 19–25
 47. Mirza, R. E., and Koh, T. J. (2015) Contributions of cell subsets to cytokine production during normal and impaired wound healing. *Cytokine* **71**, 409–412
 48. Anderson, K., and Hamm, R. L. (2014) Factors that impair wound healing. *J. Am. Coll. Clin. Wound Spec.* **4**, 84–91
 49. Guo, J. J., Yang, H., Qian, H., Huang, L., Guo, Z., and Tang, T. (2010) The effects of different nutritional measurements on delayed wound healing after hip fracture in the elderly. *J. Surg. Res.* **159**, 503–508
 50. Falanga, V. (2005) Wound healing and its impairment in the diabetic foot. *Lancet* **366**, 1736–1743
 51. Dinarello, C. A. (2000) Proinflammatory cytokines. *Chest* **118**, 503–508
 52. Efron, P. A., and Moldawer, L. L. (2004) Cytokines and wound healing: the role of cytokine and anticytokine therapy in the repair response. *J. Burn Care Rehabil.* **25**, 149–160
 53. Taylor, P. R., and Gordon, S. (2003) Monocyte heterogeneity and innate immunity. *Immunity* **19**, 2–4
 54. Kimball, A., Schaller, M., Joshi, A., Davis, F. M., denDekker, A., Boniakowski, A., Bermick, J., Obi, A., Moore, B., Henke, P. K., Kunkel, S. L., and Gallagher, K. A. (2018) Ly6C^{hi} blood monocyte/macrophage drive chronic inflammation and impair wound healing in diabetes mellitus. *Arterioscler. Thromb. Vasc. Biol.* **38**, 1102–1114
 55. Geissmann, F., Jung, S., and Littman, D. R. (2003) Blood monocytes consist of two principal subsets with distinct migratory properties. *Immunity* **19**, 71–82
 56. Lin, S. L., Castaño, A. P., Nowlin, B. T., Lupher, M. L., Jr., and Duffield, J. S. (2009) Bone marrow Ly6C^{high} monocytes are selectively recruited to injured kidney and differentiate into functionally distinct populations. *J. Immunol.* **183**, 6733–6743
 57. Ramachandran, P., Pellicoro, A., Vernon, M. A., Boulter, L., Aucott, R. L., Ali, A., Hartland, S. N., Snowden, V. K., Cappon, A., Gordon-Walker, T. T., Williams, M. J., Dunbar, D. R., Manning, J. R., van Rooijen, N., Fallowfield, J. A., Forbes, S. J., and Iredale, J. P. (2012) Differential Ly6C expression identifies the recruited macrophage phenotype, which orchestrates the regression of murine liver fibrosis. *Proc. Natl. Acad. Sci. USA* **109**, E3186–E3195
 58. Autengruber, A., Gereke, M., Hansen, G., Hennig, C., and Bruder, D. (2012) Impact of enzymatic tissue disintegration on the level of surface molecule expression and immune cell function. *Eur. J. Microbiol. Immunol. (Bp.)* **2**, 112–120
 59. Menke, N. B., Ward, K. R., Witten, T. M., Bonchev, D. G., and Diegelmann, R. F. (2007) Impaired wound healing. *Clin. Dermatol.* **25**, 19–25
 60. Couper, K. N., Blount, D. G., and Riley, E. M. (2008) IL-10: the master regulator of immunity to infection. *J. Immunol.* **180**, 5771–5777
 61. Murray, P. J. (2005) The primary mechanism of the IL-10-regulated anti-inflammatory response is to selectively inhibit transcription. *Proc. Natl. Acad. Sci. USA* **102**, 8686–8691

62. Isomaki, P., Luukkainen, R., Saario, R., Toivanen, P., and Punnonen, J. (1996) Interleukin-10 functions as an antiinflammatory cytokine in rheumatoid synovium. *Arthritis Rheum.* **39**, 386–395
63. Vieira, P., de Waal-Malefyt, R., Dang, M. N., Johnson, K. E., Kastelein, R., Fiorentino, D. F., de Vries, J. E., Roncarolo, M. G., Mosmann, T. R., and Moore, K. W. (1991) Isolation and expression of human cytokine synthesis inhibitory factor cDNA clones: homology to Epstein-Barr virus open reading frame BCRF1. *Proc. Natl. Acad. Sci. USA* **88**, 1172–1176
64. Martin, P. (1997) Wound healing—aiming for perfect skin regeneration. *Science* **276**, 75–81
65. McDonald, P. P., Fadok, V. A., Bratton, D., and Henson, P. M. (1999) Transcriptional and translational regulation of inflammatory mediator production by endogenous TGF-beta in macrophages that have ingested apoptotic cells. *J. Immunol.* **163**, 6164–6172
66. Zdrengeha, M. T., Makrinioti, H., Muresan, A., Johnston, S. L., and Stanciu, L. A. (2015) The role of macrophage IL-10/innate IFN interplay during virus-induced asthma. *Rev. Med. Virol.* **25**, 33–49
67. Ortega-Gómez, A., Perretti, M., and Soehnlein, O. (2013) Resolution of inflammation: an integrated view. *EMBO Mol. Med.* **5**, 661–674
68. Gjødsbøl, K., Christensen, J. J., Karlsmark, T., Jørgensen, B., Klein, B. M., and Kroghfelt, K. A. (2006) Multiple bacterial species reside in chronic wounds: a longitudinal study. *Int. Wound J.* **3**, 225–231
69. Lai, Y., and Gallo, R. L. (2009) AMPed up immunity: how antimicrobial peptides have multiple roles in immune defense. *Trends Immunol.* **30**, 131–141
70. Joo, H. S., and Otto, M. (2012) Molecular basis of *in vivo* biofilm formation by bacterial pathogens. *Chem. Biol.* **19**, 1503–1513
71. Guaní-Guerra, E., Santos-Mendoza, T., Lugo-Reyes, S. O., and Terán, L. M. (2010) Antimicrobial peptides: general overview and clinical implications in human health and disease. *Clin. Immunol.* **135**, 1–11
72. Chung, P. Y., and Khanum, R. (2017) Antimicrobial peptides as potential anti-biofilm agents against multidrug-resistant bacteria. *J. Microbiol. Immunol. Infect.* **50**, 405–410
73. Izadpanah, A., and Gallo, R. L. (2005) Antimicrobial peptides. *J. Am. Acad. Dermatol.* **52**, 381–390; quiz 391–392
74. Ganz, T. (2003) Defensins: antimicrobial peptides of innate immunity. *Nat. Rev. Immunol.* **3**, 710–720
75. Brogden, K. A. (2005) Antimicrobial peptides: pore formers or metabolic inhibitors in bacteria? *Nat. Rev. Microbiol.* **3**, 238–250
76. Yang, D., Chertov, O., and Oppenheim, J. J. (2001) The role of mammalian antimicrobial peptides and proteins in awakening of innate host defenses and adaptive immunity. *Cell. Mol. Life Sci.* **58**, 978–989
77. Nizet, V., Ohtake, T., Lauth, X., Trowbridge, J., Rudisill, J., Dorschner, R. A., Pestonjamas, V., Piraino, J., Huttner, K., and Gallo, R. L. (2001) Innate antimicrobial peptide protects the skin from invasive bacterial infection. *Nature* **414**, 454–457
78. Howard, O. M., Dong, H. F., Yang, D., Raben, N., Nagaraju, K., Rosen, A., Casciola-Rosen, L., Härtle, M., Kron, M., Yang, D., Yadom, K., Dwivedi, S., Plotz, P. H., and Oppenheim, J. J. (2002) Histidyl-tRNA synthetase and asparaginyl-tRNA synthetase, autoantigens in myositis, activate chemokine receptors on T lymphocytes and immature dendritic cells. *J. Exp. Med.* **196**, 781–791
79. Yang, D., Chertov, O., Bykovskaia, S. N., Chen, Q., Buffo, M. J., Shogan, J., Anderson, M., Schröder, J. M., Wang, J. M., Howard, O. M., and Oppenheim, J. J. (1999) Beta-defensins: linking innate and adaptive immunity through dendritic and T cell CCR6. *Science* **286**, 525–528
80. Wolf, M., and Moser, B. (2012) Antimicrobial activities of chemokines: not just a side-effect? *Front. Immunol.* **3**, 213
81. Huang, L. C., Redfern, R. L., Narayanan, S., Reins, R. Y., and McDermott, A. M. (2007) *In vitro* activity of human beta-defensin 2 against *Pseudomonas aeruginosa* in the presence of tear fluid. *Anti-microb. Agents Chemother.* **51**, 3853–3860
82. Chen, H., Wubbolts, R. W., Haagsman, H. P., and Veldhuizen, E. J. A. (2018) Inhibition and eradication of *Pseudomonas aeruginosa* biofilms by host defence peptides. *Sci. Rep.* **8**, 10446
83. Moser, C., Weiner, D. J., Lysenko, E., Bals, R., Weiser, J. N., and Wilson, J. M. (2002) Beta-defensin 1 contributes to pulmonary innate immunity in mice. *Infect. Immun.* **70**, 3068–3072
84. Morrison, G., Kilanowski, F., Davidson, D., and Dorin, J. (2002) Characterization of the mouse beta defensin 1, Defb1, mutant mouse model. *Infect. Immun.* **70**, 3053–3060
85. Lim, S. Y., Raftery, M. J., and Geczy, C. L. (2011) Oxidative modifications of DAMPs suppress inflammation: the case for S100A8 and S100A9. *Antioxid. Redox Signal.* **15**, 2235–2248
86. Hsu, K., Champaiboon, C., Guenther, B. D., Sorenson, B. S., Khammanivong, A., Ross, K. F., Geczy, C. L., and Herzberg, M. C. (2009) Anti-infective protective properties of S100 calgranulins. *Antiinflamm. Antiallergy Agents Med. Chem.* **8**, 290–305
87. Edwards, H., Finlayson, K., Courtney, M., Graves, N., Gibb, M., and Parker, C. (2013) Health service pathways for patients with chronic leg ulcers: identifying effective pathways for facilitation of evidence based wound care. *BMC Health Serv. Res.* **13**, 86
88. Bosanquet, D. C., and Harding, K. G. (2014) Wound duration and healing rates: cause or effect? *Wound Repair Regen.* **22**, 143–150
89. Järbrink, K., Ni, G., Sönnergren, H., Schmidtchen, A., Pang, C., Bajpai, R., and Car, J. (2016) Prevalence and incidence of chronic wounds and related complications: a protocol for a systematic review. *Syst. Rev.* **5**, 152
90. Ireton, J. E., Unger, J. G., and Rohrich, R. J. (2013) The role of wound healing and its everyday application in plastic surgery: a practical perspective and systematic review. *Plast. Reconstr. Surg. Glob. Open* **1**, e10–e19
91. Held, M., Rothenberger, J., Tolzmann, D., Petersen, W., Schaller, H. E., and Rahmanian-Schwarz, A. (2015) Alteration of biomechanical properties of skin during the course of healing of partial-thickness wounds. *Wounds* **27**, 123–128
92. Yates, C. C., Hebda, P., and Wells, A. (2012) Skin wound healing and scarring: fetal wounds and regenerative restitution. *Birth Defects Res. C Embryo Today* **96**, 325–333
93. Tomasek, J. J., Gabbiani, G., Hinz, B., Chaponnier, C., and Brown, R. A. (2002) Myofibroblasts and mechano-regulation of connective tissue remodelling. *Nat. Rev. Mol. Cell Biol.* **3**, 349–363
94. Hurme, T., Kalimo, H., Sandberg, M., Lehto, M., and Vuorio, E. (1991) Localization of type I and III collagen and fibronectin production in injured gastrocnemius muscle. *Lab. Invest.* **64**, 76–84
95. Singer, A. J., and Clark, R. A. (1999) Cutaneous wound healing. *N. Engl. J. Med.* **341**, 738–746

Received for publication February 21, 2018.
Accepted for publication August 27, 2018.